

Lightweight alkali activated composites by direct foaming based on ceramic tile waste and fly ash

Giulia Masi^{*}, Alessandro Tugnoli, Maria Chiara Bignozzi

Department of Civil, Chemical, Environmental and Materials Engineering, University of Bologna, via Terracini 28, 40131, Bologna, Italy

ARTICLE INFO

Handling Editor: Dr P. Vincenzini

Keywords:

Foam
Alkali activated material
Thermal conductivity
Expanded perlite
Ceramic tile waste

ABSTRACT

This study aims at investigating for the first time if ceramic waste coming from the rectifying process of porcelain stoneware tiles are suitable to prepare alkali activated lightweight composites. After successfully designing alkali activated materials based on ceramic waste, different foaming agents were added alone or in combination with sodium dodecyl sulfate acting as pore stabilizing agent. Addition of expanded perlite as lightweight constituent was also tested. Different properties, such as geometric density, water absorption, porosity and pore size distribution by mercury intrusion porosimetry and SEM observations, and thermal conductivity, were measured in view of their potential future applications. The results highlight that combining ceramic tile waste as raw materials, hydrogen peroxide as foaming agent, sodium dodecyl sulfate as pore stabilizing agent and expanded perlite allow the preparation of optimized lightweight composites with a density of 0.75 g/cm³, a water absorption greater than 70 % and a thermal conductivity of 0.26 W/mK.

1. Introduction

One of the major potentialities of alkali activated materials is the possibility of using a wide range of precursors derived from industrial by-products. Many varieties of metallurgical, building sector and agriculture wastes can be applied as promising raw materials for alkali activation or at least as SiO₂ source [1,2]. In addition, to valorize the environmental sustainability of these materials, one route is to use locally available waste [3]. This choice would minimize the transport of bulk materials that is a component that often dominates the emission impacts in LCA environmental analysis [3,4]. Among the others, ceramic-type wastes represent promising precursors for alkali activation. This waste category has been widely used to produce more sustainable construction materials, such as foam ceramics, concrete and ceramic tiles [5,6]. Ceramic-type wastes can be sourced from construction and demolition (C&D) waste (including concrete, bricks, roof tiles and ceramic materials in general) or from ceramic industry processes (waste from production of bricks, tiles and refractories) [1,7]. Ceramic waste from C&D operations shows some important challenges due to the complexity to use selective separation procedures. Current separation usually leads to ceramic waste with heterogenous compositions and a large presence of contaminants, such as glass, wood, gypsum [8], that do not allow an efficient recycling as raw materials for alkali

activation. On the contrary, ceramic waste directly generated by industry is potentially more easily recyclable in alkali activation thanks to a major control of origin and composition. Indeed, previous studies have demonstrated the suitability of clay brick powders-based waste [9–12] and mixed ceramic waste [7,13–15] as precursors for alkali activation. Other studies have also demonstrated the applicability of refractory waste as fillers for enhancing high temperature properties of alkali activated materials [16,17]. Other studies have explored the mechanical improvement of alkali activated mortars thanks to the replacement of fine aggregates with ceramic waste [18,19]. Even if some ceramic tiles waste is already successfully involved in a close-loop recycling [20,21], it shall be reminded that world ceramic tile production is huge (about 16,800 million m² in 2022 [22]), thus ceramic tiles waste remains an interesting potential source. Spain and Italy are the largest European producers of ceramic tiles: they were at the 5th and 7th places of the global ceramic tile manufacturers with a total production of 500 and 431 million of m² in 2022, respectively, corresponding to the 3.0 and 2.6 % of the world production [22]. Thus, ceramic tile waste can be largely available in Europe, especially in Valencia and Emilia-Romagna regions, where the two most important European ceramic clusters are located (Castellon in Spain and Sassuolo/Fiorano Modenese in Italy).

A successful application for alkali activated materials is the synthesis of highly porous materials by foam preparation. In general, these

^{*} Corresponding author.

E-mail address: giulia.masi5@unibo.it (G. Masi).

<https://doi.org/10.1016/j.ceramint.2024.10.399>

Received 30 August 2024; Received in revised form 18 October 2024; Accepted 27 October 2024

Available online 28 October 2024

0272-8842/© 2024 The Authors. Published by Elsevier Ltd. This is an open access article under the CC BY license (<http://creativecommons.org/licenses/by/4.0/>).

materials exhibit high porosity values, moderate mechanical properties and low thermal conductivity values that are dependent to their porosity development [23–25]. The synthesis of low-density alkali activated materials represents a challenge and an optimized procedure shall be investigated for each different foaming technique: small pore size and uniform pore distribution needs to be achieved and pore collapse should be avoided. Different approaches can be pursued such as chemical foaming technique, direct addition of gas bubbles, extraction of sacrificial fillers, replica methods, or additive manufacturing [24–27]. The most common synthesis process is the addition of a foaming agent that reacts in-situ and produces gas bubbles that remain entrapped in the matrix [24,26]. The effect of the addition of several foaming agents have already been investigated in alkali activated materials mainly prepared with the commonly used precursors, such as metakaolin, slags and fly ash [27]. Hydrogen peroxide, metallic powders (e.g. Al and Si powders), agents containing Si (e.g. silica fume, Si and FeSi-based alloy) and sodium perborate are the main investigated agents [28–33]. Addition of Al powder to fly ash-based geopolymers leads to density of 0.4–0.8 g/cm³, however mainly closed pores are formed [31]. Moreover, it was found that increasing aluminum concentration, coarse and non-homogenously distributed porosity is obtained [30,32,34]. While using 0.1 wt% hydrogen peroxide leads to a homogeneously distributed porosity of macro-pores, increasing H₂O₂ concentrations leads to pore coalescence in fly ash-based geopolymers [30]. In order to optimize the performance of the mentioned foaming agents, a promising approach is to add in combination pore stabilizing agents (surfactants) such as commercial products (Tween80, TritonX-100, Sika Lightcrete02) or sodium dodecyl sulfate (SDS) [30,35–37]. Indeed, high porosity and homogenous pore distribution are reached, especially when surfactant and foaming agent are added in equal concentrations [36]. Moreover, to enhance the porosity of alkali activated foams, addition of lightweight constituents can also be pursued. In literature, different lightweight materials derived from natural resources (perlite, pumice, shale, ceramics and slate sand all in the expanded forms) or from industrial wastes (recycled lightweight blocks, expanded glass and recycled thermosetting and thermoplastic materials) were successfully added to alkali activated matrices [24,38,39].

This paper presents two main goals. The first one is to assess if ceramic tile waste coming from the rectification process of porcelain stoneware tiles is a suitable precursor to be alkali activated. The interest for this type of waste, never tested so far by alkali activation, is based on the fact that porcelain stoneware tiles are currently considered the top-quality ceramic tile in Europe and the rectification process is practically a mandatory step. A production of about 2 million of tons of this waste can be expected only in Europe. The second goal is to obtain lightweight composites with an open porosity greater than 50 % and a thermal conductivity lower than 0.30 W/mK by means of foaming process optimization and addition of expanded perlite. Lightweight composites with these target characteristics can be employed in the building engineering sector as thermal insulation (e.g. production of foamed blocks with enhanced thermal insulation properties) and/or fireproofing materials [30,31].

Both the above-mentioned goals are challenging and unexplored at the best of our knowledge. The most recent studies involving ceramic wastes regards ceramic waste pottery [15] as partial replacement of fly ash, and ceramic waste as fine aggregates to produce alkali activated mortars [19]. In addition, research results on different types of ceramic waste used for geopolymers synthesis [20] and on anti-bacterial alkali activated cement based on white ceramic waste [40] were also published. Ceramic waste (i.e., coming from ceramic tiles, bricks and sanitary) was also applied to produce sustainable cements and concrete [41], bedding mortars for Cultural Heritage conservation [42], and materials for high temperature applications [43]. Moreover, Liang et al. developed lightweight aggregates for concrete by expanding, pelletizing and granulating ceramic tile waste [44].

To reach the two main objectives of this research, investigations have

been developed by (i) designing alkali activated mixes based on different content of ceramic waste; (ii) optimizing different direct foaming methods tested alone and in combination with a pore stabilizing agent; (iii) evaluating the effect of different amount of expanded perlite addition in the most porous samples, in order to produce lightweight composites. As early-curing temperature is a critical parameter in porosity development of alkali activated composites [45,46], its influence has been also investigated maintaining it always lower than 100 °C.

2. Methods

2.1. Materials

Ceramic waste (CW) (kindly supplied by Italcerc group – Ceramica Rondine (Rubiera, RE, Italy) coming from industrial rectifying procedure of porcelain stoneware tiles, was selected as precursor for alkali activation. This waste was used as supplied without any pre-treatment because it was already a fine powder. CW exhibits a d(50) of 20.3 μm, as determined by laser granulometry, a density of 2.43 ± 0.01 g/cm³, as measured by water pycnometer, and a specific surface of 3610 cm²/g as determined by N₂ adsorption technique at 77 K (and application of BET equation). SEM observation, reported in Fig. 1, shows angular shape for CW particles.

CW chemical composition, determined by ICP-OES (PerkinElmer, Avio 550 MAX), is reported in Table 1 and exhibits SiO₂ and Al₂O₃ as main oxides with a content of 73.2 and 17.5 wt%, respectively. Quantitative mineralogical analysis, carried out by a Philips PW 1280 diffractometer (equipped with a Cu-Kα (1.5406 Å) radiation source and excited with 30 mA and 40 kV) and obtained by Rietveld refinement to obtain quantitative data, shows that CW contains 69.4 ± 1.4 wt% of amorphous phase, 22.1 ± 0.1 wt% of quartz, 4.0 ± 0.4 wt% of mullite, 3.5 ± 0.4 wt% of plagioclase and minor phases (<1.0 wt%) such as silicon carbide, cristobalite and zircon. Such impurities are mainly due to abrasive wheels used for tile rectification process.

To optimize the mix design of alkali activated materials based on CW, fly ash (FA) was used as co-precursor, being one of the most reactive raw materials, besides metakaolin [29,39,47]. Low-calcium fly ash (Class F according to ASTM C618 standard) sourced by BauMineral (EFA-Fuller®) was selected and its chemical composition is reported in previous studies [48,49]. Density of FA is equal to 2.4 g/cm³ [50], and a specific surface of 2220 cm²/g was measured by N₂ adsorption technique at 77 K (and application of BET equation).

For alkali activation, 8M sodium hydroxide (NaOH) and sodium silicate solutions were used. 320 g NaOH pellets (ACS reagent, 97 %) supplied by Sigma Aldrich were dissolved in 1L of deionized water to obtain the 8M concentration. Sodium silicate solution, supplied by Ingessil S.r.l (Italy), has a SiO₂/Na₂O ratio equal to 2.07 and shows a

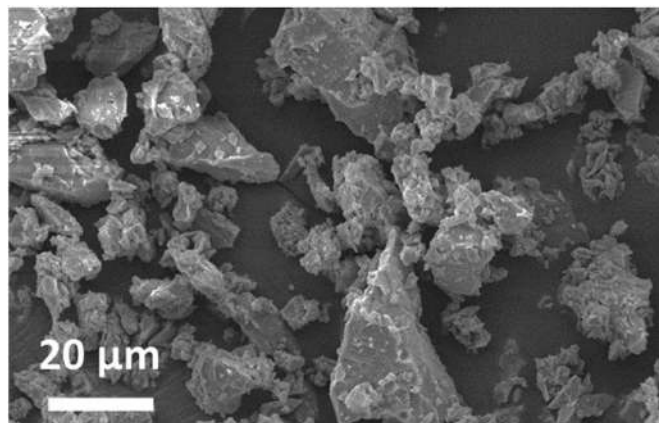


Fig. 1. CW observation by SEM.

Table 1

Chemical composition (wt%) of ceramic waste (CW) measured by ICP-OES (LOI = Loss of Ignition).

| SiO ₂ | Al ₂ O ₃ | TiO ₂ | Fe ₂ O ₃ | CaO | MgO | K ₂ O | Na ₂ O | ZrO ₂ | SO ₃ | LOI |
|------------------|--------------------------------|------------------|--------------------------------|-----|-----|------------------|-------------------|------------------|-----------------|-----|
| 73.2 | 17.5 | 0.8 | 1.1 | 1.5 | 0.5 | 1.9 | 2.9 | 0.4 | 0.1 | 0.4 |

composition of 29.9 % SiO₂, 14.4 % Na₂O and 55.7 % H₂O.

To prepare foams, a pore stabilizing agent (surfactant) and three foaming agents were tested varying their content. For each agent, different ranges of concentration have been selected. The maximum concentration was set by preliminary screening tests in order to avoid pore coalescence phenomena. In particular, the following agents were used:

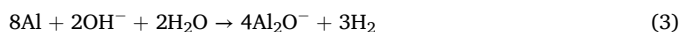
- sodium dodecyl sulfate (SDS, MP Biomedicals ultrapure, ≥99.9 %) as anionic surfactant in the form of white powder. It was added in the mix in amount ranging from the 0.5 to 2.5 wt%;
- hydrogen peroxide (HP, Sigma Aldrich) as foaming agent: a 30 vol% solution was added in the mix in amount ranging from 0.5 to 2.5 wt %. It is well known that hydrogen peroxide acts as chemical blowing agent forming oxygen gas, according to Eq. (1) [30]:



- sodium bicarbonate (SB, Crastan S.p.A) as a foaming agent in the form of white powder. It was added in the mix in amount ranging from 5 to 10 wt%. This blowing agent is currently used to prepare low density polymeric materials [51,52], as sodium bicarbonate decomposes for temperature equal or greater of 100 °C producing carbon dioxide (CO₂) gas in accordance with Eq. (2) [52]:



- metallic aluminum (Al) as a foaming agent: it was obtained by manually chopping exhausted coffee capsules for automatic coffee machines. After chopping, Al particles smaller than 5 mm (Fig. S1 in the Supplementary Materials section) were rinsed with water to eliminate coffee residues. Al scraps were added in the mix in amount ranging from 0.2 to 1.0 wt%. The effect of metallic aluminum as blowing agent is related to hydrogen gas formation due to the basic environment obtain by alkaline solutions, following Eq. (3) [30]:



The use of recycled aluminum scraps as foaming agent has been selected on purpose in view to develop waste-based material with a circular economy approach.

Expanded perlite (supplied by Perlite Italiana) with a fixed grain size distribution and $d_{\text{max}} = 2$ mm was also added in different content (5, 10 and 13 wt%) to prepare lightweight composites. It exhibits a density of 0.7–0.9 g/cm³, according to technical data sheet. The maximum amount of expanded perlite added, i.e., 13 wt%, was selected on the basis of the results of a previous study that demonstrated this concentration is the maximum to obtain acceptable workability without modifying the water content [38].

2.2. Mix designs and sample preparation

Different formulations were prepared using different content of CW and FW as precursor and co-precursor, respectively. Table 2 reports the mix design (in wt%): the sample code represents the amount of CW used as precursor (25, 50, 75 and 100 %). As reference sample, a mix design with 100 % fly ash (OCW) was also prepared and tested. All the mix designs are based on the same theoretical molar ratios for alkali activation: Si/Al = 2.5, Na/Al = 1.0, Na/Si = 0.4. A target workability of 80 ± 2 mm diameter of slurry by flow test, using a mini-cone slump tester with the following dimensions: H = 57 mm, D_{TOP} = 19 mm and D_{BOTTOM}

Table 2

Mix design (wt%) of the investigated samples.

| Sample | FA | CW | 8M NaOH solution | Sodium silicate solution | Extra H ₂ O |
|--------|------|------|------------------|--------------------------|------------------------|
| 0CW | 71.3 | – | 22.5 | 6.2 | – |
| 25CW | 53.2 | 17.7 | 21.3 | 6.4 | 1.4 |
| 50CW | 34.6 | 34.6 | 20.1 | 5.9 | 4.8 |
| 75CW | 16.9 | 50.6 | 18.9 | 5.4 | 8.3 |
| 100CW | – | 66.3 | 17.9 | 4.6 | 11.2 |

= 38 mm, has been adopted according to previous experience [31]. Workability target was set to minimize air entrapment especially when lightweight aggregates have been used. Increasing the CW content, the addition of extra water was required compared to sample based on 100 % FA (OCW).

Samples were prepared by dry mixing the precursors. Then, alkaline solutions were added, and the mixing proceeded for 1 min and 30 s. When necessary (in agreement with Table 2), deionized water was added and an additional mixing for 1 min and 30 s was carried out. The mix was then poured into cylindrical samples (35 mm diameter and 20 mm height). All the samples were cured in sealed conditions wrapped in a close plastic bag at different curing temperature for 24 h: room temperature (RT, 23 ± 2 °C), 50 and 80 °C. After one day of curing, samples were demolded and stored in sealed condition for further 6 days at room temperature. For each mix, 5 cylindrical samples were prepared for testing.

2.3. Foam sample preparation

Foam samples were prepared in accordance with the mix designs reported in Table 3: 100CW has been selected as un-foam sample reference and it was used as base for the addition of different content of surfactant or foaming agents. Foam samples have been named “F”, followed by the content (wt%) and the acronym of the surfactant (SDS) or the foaming agents (HP, SB and Al).

To investigate the potentiality of SDS as foam stabilizing agent, combination of SDS and HP were also tested by maintaining constant the concentration of HP at 1.0 wt% and ranging the concentration of SDS between 0.5 and 2.0 wt%, as reported in Table 4. This set of samples have been named “HP”, followed by the content and surfactant acronym (SDS).

Foam samples were prepared following the procedure reported in paragraph 2.2: after the 3 min mixing, surfactant or the foaming agents or the combination of SDS and HP were added, and additional mixing was performed for 30 s. Then the mix was poured in cylindrical samples (35 mm diameter and 20 mm height) and cured in sealed condition wrapped in a close plastic bag. Curing temperature was 50 °C for 24 h for all the mixes excepts for mixes containing sodium bicarbonate that were cured at 100 °C for 24 h to promote sodium carbonate decomposition. Foam samples were then demolded and stored in sealed condition for further 6 days at room temperature, before testing.

2.4. Lightweight composite preparation

Lightweight composites have been prepared after the selection of the most promising foaming agents. For this reason, a combination of SDS and HP added in the same concentration (1.0 wt%) was selected. By increasing the expanded perlite content, extra water was added to achieve a targeted workability in accordance with EN 1015-3 (160 mm

Table 3

Mix design (wt%) of the foam samples obtained by adding different concentrations of sodium dodecyl sulfate (SDS), hydrogen peroxide (HP), sodium bicarbonate (SB) and metallic aluminum (Al) obtained by manually chopping of exhausted coffee capsules.

| Sample | CW | 8 M NaOH solution | Sodium silicate solution | H ₂ O | Foaming agent |
|----------|------|-------------------|--------------------------|------------------|---------------|
| F-0.5SDS | 66.0 | 17.8 | 4.6 | 11.1 | 0.5 |
| F-1.0SDS | 65.6 | 17.7 | 4.6 | 11.1 | 1.0 |
| F-1.5SDS | 65.3 | 17.6 | 4.6 | 11.0 | 1.5 |
| F-2.0SDS | 65.0 | 17.5 | 4.6 | 10.9 | 2.0 |
| F-2.5SDS | 64.6 | 17.4 | 4.5 | 10.9 | 2.5 |
| F-0.5HP | 65.9 | 17.8 | 4.6 | 11.1 | 0.5 |
| F-1.0HP | 65.6 | 17.7 | 4.5 | 11.1 | 1.0 |
| F-1.5HP | 65.3 | 17.6 | 4.5 | 11.0 | 1.5 |
| F-2.0HP | 65.0 | 17.5 | 4.5 | 10.9 | 2.0 |
| F-2.5HP | 64.6 | 17.4 | 4.5 | 10.9 | 2.5 |
| F-5.0SB | 63.0 | 17.0 | 4.4 | 10.6 | 5.0 |
| F-7.5SB | 61.3 | 16.6 | 4.29 | 10.4 | 7.5 |
| F-10SB | 59.6 | 16.1 | 4.18 | 10.1 | 10.0 |
| F-0.2Al | 66.2 | 17.9 | 4.63 | 11.2 | 0.2 |
| F-0.4Al | 66.0 | 17.8 | 4.62 | 11.1 | 0.4 |
| F-0.6Al | 65.9 | 17.8 | 4.61 | 11.1 | 0.6 |
| F-0.8Al | 65.8 | 17.7 | 4.60 | 11.1 | 0.8 |
| F-1.0Al | 65.6 | 17.7 | 4.59 | 11.1 | 1.0 |

Table 4

Mix design (wt%) of the foam samples (HP) prepared with a constant amount of 1.0 wt% of HP, varying SDS in the range of 0.5–2.0 wt% and of lightweight mortars (M) obtained by the addition of expanded perlite (5, 10 and 13 wt%) and a combination of SDS and HP (both at 1.0 wt%).

| Sample | CW | Expanded perlite | 8 M NaOH solution | Sodium silicate solution | H ₂ O | SDS | HP |
|-----------|------|------------------|-------------------|--------------------------|------------------|-----|-----|
| HP-0.5SDS | 65.3 | – | 17.6 | 4.6 | 11.0 | 0.5 | 1.0 |
| HP-1.0SDS | 65.0 | – | 17.5 | 4.6 | 10.9 | 1.0 | 1.0 |
| HP-1.5SDS | 64.6 | – | 17.5 | 4.5 | 10.9 | 1.5 | 1.0 |
| HP-2.0SDS | 64.3 | – | 17.4 | 4.5 | 10.9 | 2.0 | 1.0 |
| M-5EP | 61.9 | 4.8 | 16.7 | 4.3 | 10.5 | 1.0 | 1.0 |
| M-10EP | 54.9 | 9.3 | 14.8 | 3.8 | 15.5 | 1.0 | 1.0 |
| M-13EP | 49.7 | 12.1 | 13.6 | 3.5 | 19.1 | 1.0 | 1.0 |

of minimum spread value) [53]. Table 4 reports the composite mix design: samples were named “M”, followed by the content and the acronym of expanded perlite (EP). Composite preparation was carried out as follows: CW and expanded perlite were manually pre-mixed and then poured in a Hobart mixer where the alkaline solutions were added. After mixing for 90 s, water was gradually added and mixed for additional 180 s. After a pause of 60 s, a combination of SDS and HP solution, was added and mixed for further 30 s. The mix was then poured in 5 cylindrical samples and in 2 slabs (90 × 90 × 30 mm), and cured at 50 °C for 24 h wrapped in a close plastic bag. After one day of curing, samples were demolded and stored in sealed condition for further 6 days at room temperature, before testing.

2.5. Characterization

Geometric density was obtained by dividing the dry mass to the volume of the cylindrical samples (35 mm diameter and 20 mm height). Due to the expected high porosity and in some cases large pore size for foams and lightweight composites, water absorption was determined under vacuum conditions in order to have a more precise evaluation [30, 38]. Dry samples (m_d) were placed under vacuum chamber for 30 min. Then, addition of deionized water in the vacuum chamber was carried out until complete sample saturation. After maintaining the vacuum level for additional 30 min, samples were weighed in saturated surface-dry condition (m_{ssd}). Saturated surface-dry weight was repeated for longer times to be sure that complete saturation of samples was reached (mass variation <0.1 %) Water absorption values were calculated as percentage of the difference between m_{ssd} and m_d divided by m_d . Both density and water absorption data are reported as average of at least three measurements.

Weight stability was evaluated by measuring the mass loss by immersing dried samples (m_d) in deionized water for 24 h. After

immersion, samples were dried at 105 ± 5 °C for 24 h and mass values were recorded (m_i). Weight stability was calculated as percentage of the difference of m_d and m_i divided by m_d . This parameter demonstrates the hydraulicity of the binder due to geopolymer formation. When a low value of mass loss is recorded (i.e. [54 NEW]), a satisfying quality of the developed alkali activated material is generally achieved.

As water absorption gives an indication of the total open porosity, mercury intrusion porosimetry (MIP) analysis allows to measure the pore size distribution under 100 μ m.

MIP measurements (Thermo Scientific Pascal 140 and 240 Mercury Porosimeters instruments) were carried out onto 1 cm³ samples avoiding the external sample surfaces. Instrument parameter of Hg contact angle (θ) equal to 141.3°, Hg surface tension (γ) of 0.48 N/m and applied pressure from 0.1 kPa to 200 MPa were applied for all the measurements and the results were managed by S.O.L.I.D. software (SOLver of Intrusion Data, Thermo Scientific).

Samples microstructure was observed by Scanning Electron Microscopy (SEM, Philips XL20) applying 10 keV and the secondary electron (SE) detector. To make the samples conductive, they were sputtered with gold before SEM observation by a Quorum sputter coater (Q150R ES). Geometric density, water absorption and weight stability and porosimetry tests, as well as SEM observation were performed after 7 days of curing.

Mechanical tests and thermal conductivity measurements were carried out on lightweight composites after 28 days of curing. Flexural (R_f) and compressive strength (R_c) were measured by an Amsler–Wolpert machine on 40 × 40 × 160 mm prismatic samples and 40 × 40 × 40 mm, respectively, applying a constant displacement rate of 5 mm/min, according to EN 196-1 [55].

A TPS1500S from Hot Disk AB equipped with Kapton-insulated sensors was used for the measurement of the effective thermal conductivity of the investigated materials. The system applies the transient

plane source technique described in ISO 22007-2 [56] and is applicable over a wide range of materials [57,58] including alkali activated materials [38]. The Hot Disk technique provides a direct measure of the thermal conductivity (k) of the material. The procedure described in ISO 22007-2 [56] was followed in the experiments and data elaboration. Sensors with 9.719 mm radius were used; the power provided to the sensor in the test was between 30 and 50 mW, the measuring time was 160 s. Two rectangular slabs (90 mm × 90 mm × 30 mm), constituted the tested samples. Each thermal conductivity result presented is the mean of measurement in three different points of the sample, each one consisting of three individual measurements with standard deviation no greater than ± 0.01 W/mK.

3. Results and discussion

3.1. Mix design optimization

The optimization of the mix design of alkali activated materials with CW as precursor has been developed adjusting ceramic tile waste content and curing temperature (RT, 50 and 80 °C). Decreasing CW concentration leads to a slight increase in geometric density and a decrease in water absorption, as shown in Fig. 2. These trends are due to a minor amount of added water in the mixes to reach the target workability and to the presence of FA as co-precursor. When only CW is present (100CW), a marked decrease in geometric density and an increase in water absorption values have been observed as function of curing temperatures.

The density and water absorption variation (−7, −11, −15 % and +26, +33, +39 %, respectively), linearly changes with the curing temperature, indicating that the best results for CW100 are obtained when RT curing is selected. Fig. 2c reports the weight stability, expressed as mass loss of the hardened samples after 24 h of water immersion. In general, increasing CW content leads to an increase in mass loss, especially for samples cured at RT and 80 °C. Weight stability (Fig. 2c), representing an index of alkali activation degree, clearly exhibits that 50 °C is the most performing curing temperature for the first 24 h for all the formulations containing at least 50 % of CW as precursor.

Moreover, samples cured at RT and 80 °C exhibit cracks, surface powdering and material loss when at least 50 % of CW as precursor was present. As already reported in the literature [46,59], elevated temperature curing plays an important role in alkali activation, also as function of the precursor nature and composition. In the Supplementary Materials section, macros of all the investigated samples are reported (Fig. S2).

These preliminary results indicate that in the investigated alkali activated system based on CW, greater variations of density and water absorption are observed compared to the ones observed for a 100 % FA system. Such a behavior can be ascribed to a higher reactivity of FA [1] compared to CW, which exhibits a different chemical composition and the presence of various crystalline phases. Moreover, particle shape of the precursor can also influence their reactivity [60]: compared to fly ash that usually exhibits mostly spherical particles [45], CW particles are characterized by angular shape, as depicted in Fig. 1. Finally, it is important to mention that to have satisfying workability, a slightly increasing content of extra water (up to 10 wt% for 100 CW) was added increasing the CW replacement (as shown in Table 2). This could promote a slight increase in porosity formation, contributing in decreasing geometric density and increasing water absorption.

3.2. Foaming optimization

Foam samples were developed on the basis of 100 wt% CW. Fig. 3 reports the physical properties (geometric density, water absorption values and pore size distribution) of the foam samples obtained by adding SDS (Fig. 3a and b), hydrogen peroxide (Fig. 3c and d), sodium bicarbonate (Fig. 3e and f) and metallic aluminum from recycled coffee

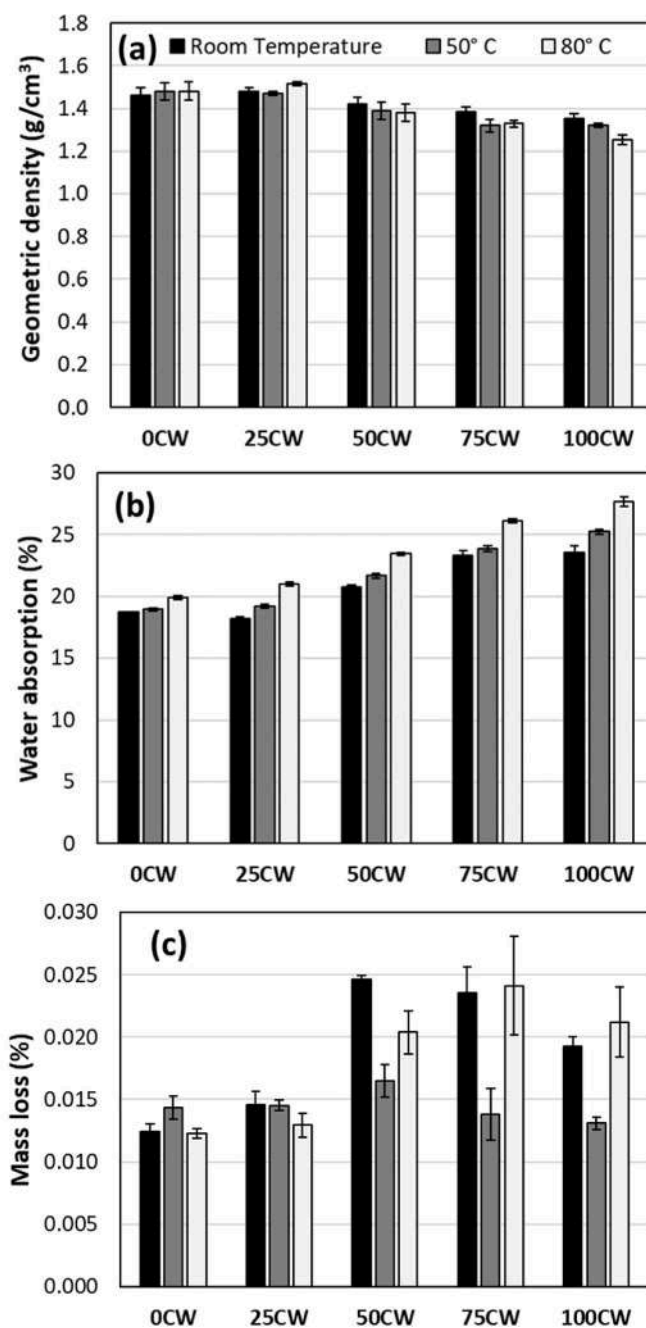


Fig. 2. (a) Geometric density, (b) water absorption values and (c) mass loss of alkali activated materials prepared by increasing content of the selected ceramic waste (CW).

capsules (Fig. 3g and h). Supplementary Materials section reports macros of the whole and cross-sectioned foam samples (Fig. S3). Addition of SDS on concentrations ranging between 0.5 and 2.5 wt%, induces only a slight effect in the foaming process. The highest SDS concentration allows a weak reduction in geometric density (about - 7 %) and a slight increase (+10 %) of water absorption, thus indicating that SDS is acting more as pore stabilizing agent than direct foaming agent, as elsewhere reported [36]. Pore size distributions (Fig. 3b), showing comparable curves corresponding to an average open porosity of 43 %, and microscopy observations, in which no macroscopic variations in porosity are evident (Fig. S3a), confirm the role of SDS.

Among the three selected foaming agents (hydrogen peroxide, sodium bicarbonate and recycled aluminum particles), HP is the one that

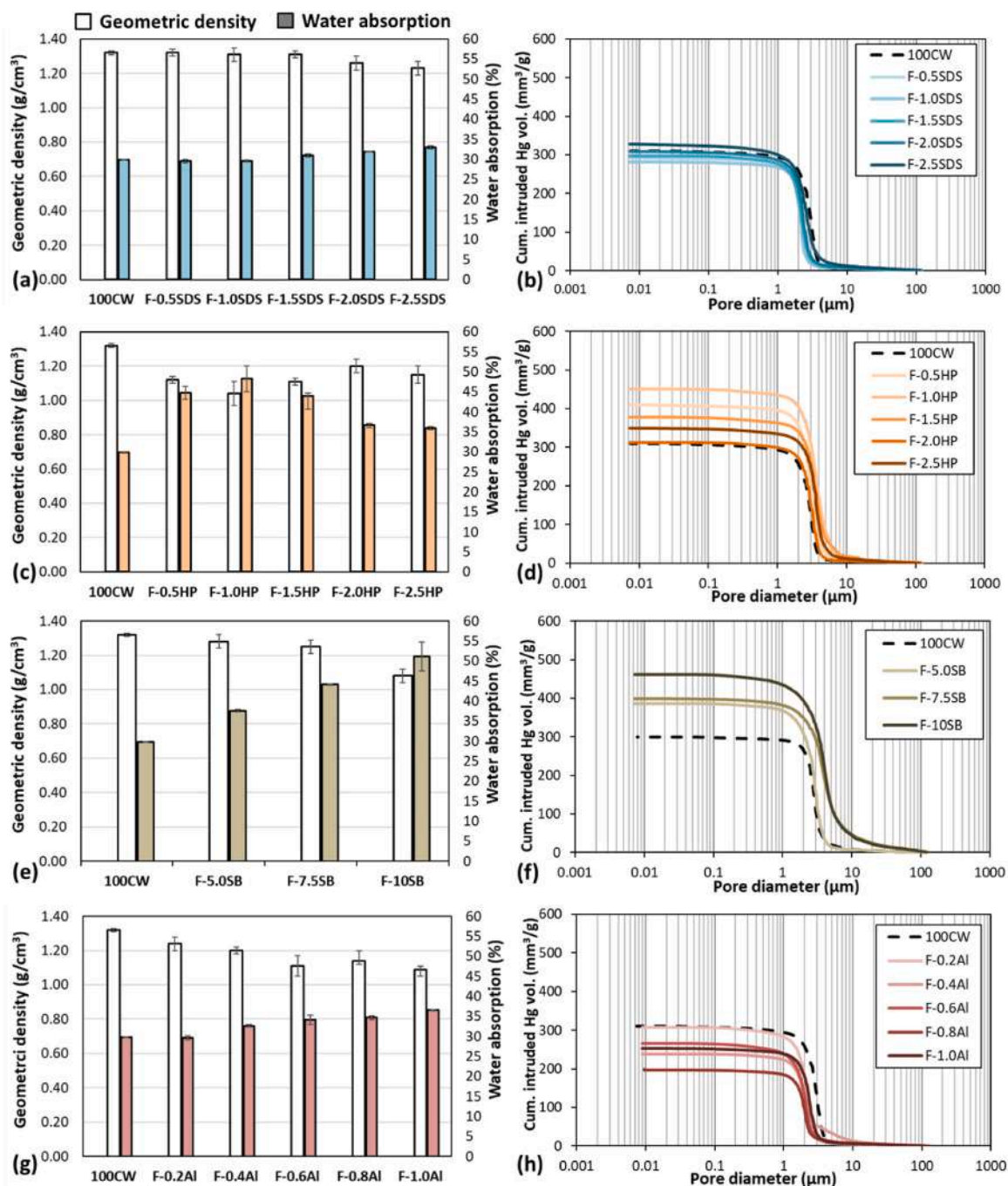


Fig. 3. Geometric density and water absorption values (on the left) and pore size distribution measured by MIP (on the right) of: (a, b) SDS, (c, d) hydrogen peroxide (HP), (e, f) sodium bicarbonate and (g, h) recycled aluminum powder.

better optimize the foaming process, especially when added in concentration of 1.0 wt%. With this amount, a geometric density of 1.04 g/cm^3 , water absorption of 48 % and a total open porosity by MIP of 53 % have been measured (Fig. 3c and Fig. S3b). For HP content >1.0 wt%, an opposite trend was observed, since density and water absorption results tend to reach the value of the un-foam reference sample (100CW). Moreover, pore size distributions (Fig. 3d) also show that samples prepared with 0.5 and 1.0 wt% of HP have intruded higher Hg volume compared to samples containing 2.0 and 2.5 wt% of HP. Such a behavior is promoted when a content of HP greater than 1.0 wt% is used, thus the tendency of pores to coalesce largely increases, as highlighted in macros reported in Fig. S3b (Supplementary Materials section). This behavior was also observed in previous studies [30,36]. Accordingly, HP

equal to 1.0 wt% has been selected as the maximum amount able to maximize the porosity and to avoid pore coalescence.

SB foaming agent has been added in the range of 5–10 wt% and with the highest amount a density of 1.08 g/cm^3 and water absorption of 51 % were determined for SB content equal to 10 wt%, as shown in Fig. 3e. Pore size distribution of SB based samples increases with SB content as reported in Fig. 3f. However, these samples exhibit a very friable structure characterized by elongated macro-pores as reported in Fig. S3c (Supplementary Materials section). In order to successfully optimize SB based samples, additional investigations are ongoing considering curing conditions at higher temperature as SB decomposes at temperatures between 100 and 180 °C. In this way, it will be possible to reduce the SB concentration, as demonstrated elsewhere [51].

Finally, the effect of the addition of recycled metallic aluminum is reported in Fig. 3g and h. The tested range did not allow an efficient foam production due to the formation of few macro-pores in correspondence of the presence of aluminum particles. This is clearly visible in Fig. S3d reported in the Supplementary Materials section. The best result was obtained by adding 1.0 wt% of Al particles that induced a density of 1.09 g/cm^3 and a water absorption value of 37 %. These results are far away from the ones obtained in other studies [24,26,29,31], in which the addition of lower concentrations (<0.1 wt%) of metallic aluminum powder leads to geometric density values lower than 0.8 g/cm^3 . The main reason for these different results is related to the aspect ratio of the added recycled aluminum particles. As the particles used in this work have been manually chopped, they are too big to ensure an effective dispersion of the pores in the alkali activated matrix as hydrogen is mainly formed at the interphase between the aluminum particles and the matrix. In order to improve the use of recycled metallic aluminum sourced from exhausted coffee capsules as foaming agent, different aspect ratios of the aluminum particles are currently under investigations.

As HP was identified as the most promising foaming agent among the tested agents, it was combined with SDS to evaluate their synergic effect in preparing foams based on the alkali activation of CW. The HP concentration was fixed at 1.0 wt% as this concentration leads to the lowest density values among the tested samples, while SDS was added in the range of 0.5–2.0 wt%. It was found that increasing the SDS concentration up to 2.0 wt%, a decrease in geometric density and a consequent increase in water absorption have been observed (Fig. 4a). In addition, the combination of the two agents promoted an increase in macro-pores ($>10 \mu\text{m}$), as observed in MIP measurements (Fig. 4b). However, samples prepared with SDS concentration greater to 1.0 wt% leads to friable samples difficult to handle (as depicted in Fig. S4 in the Supplementary Materials section). The obtained results about the combination of HP and SDS are coherent with a study by Korat and Ducman where they stated the importance of tailoring the SDS concentration on the basis of HP [36]. With the aim to better highlight the improvement due by the different agents, Fig. 5 reports the physical properties of the foams obtained by the combination of SDS and HP compared with the samples with SDS or HP alone. It is clearly observable that HP-1.0SDS shows the lowest geometric density values and the greatest porosity both in terms of water absorption and MIP results. These results are in accordance with previous studies where H_2O_2 was used in combination with an additive (e.g. pore stabilizer or surfactant) to foam fly ash-based alkali activated materials [24,30,36].

SEM observations are reported in Fig. 6. Fig. 6a shows the microstructure of the unfoam sample, characterized by the formation of a continuous gel matrix embedding some unreacted CW particles (Fig. 6b). The formation of more porous microstructure compared to FA-based one [47,49] was somehow expected due to the lower amount of amorphous phase (around 70 %) in CW. In addition, it is shown that

F-1.0SDS (Fig. 6c has a microstructure like the reference sample (100CW, Fig. 6a) except for some macro-pores due to SDS addition. Porosity increases with the addition of 1.0 wt% hydrogen peroxide (F-1.0HP, Fig. 6d) and the combination of hydrogen peroxide and SDS (HP-1.0SDS, Fig. 6e). SEM observations agreed with MIP and water absorption data, thus confirming the efficiency of the synergic action of HP and SDS system.

3.3. Lightweight composites

The effect of expanded perlite addition (up to 13 wt%) on HP-1.0SDS mix made with 100 % CW as precursor is reported in Table 5, where geometric density and water absorption values of the investigated composites are reported as function of the EP content.

Results show that increasing the expanded perlite content, a decrease in geometric density and an increase in water absorption are detected. In particular, adding 5 wt% of EP induces a slight decrease in geometric density (about 5 %) and a slight increase in water absorption. Fig. 6f reports the characteristic microstructure of the lightweight composite (M-5EP). The addition of 10 and 13 wt% of EP leads to a decrease of 25 and 32 % for geometric density and a noteworthy increase of 37 and 61 % for water absorption, respectively. These results are in accordance with the ones obtained for fly ash-based composites containing similar expanded perlite content [38,39,61].

Table 5 also reports the mechanical performances of lightweight composites, as well as their thermal conductivity. In particular, the addition of 5 and 10 % of expanded perlite induces a strong decrease in the mechanical tests. In fact, a decrease of about 21 and 56 % in R_c was respectively found. The same trend was observed for R_f that decreased of about 18 and 45 %, respectively. Comparable mechanical performances were observed for composites with 10 and 13 wt% of EP, as reported elsewhere for fly ash-based lightweight composites [36].

Concerning thermal conductivity, HP-1.0SDS shows k value around 0.48 W/(m K) , while adding EP to a lowering in thermal conductivity values up to 0.25 W/(m K) is observed. As for mechanical performances, no relevant differences in k values have been determined for composites containing 10 and 13 % of EP. Such results indicate that the addition of EP in this range allows a decrease in geometric density without affecting mechanical and thermal properties.

Finally, Fig. 7 shows the effect of different temperatures (50, 70 and $85 \text{ }^\circ\text{C}$) for the first 24h curing on the physical properties of M-5EP and M-10EP lightweight composites. These two mixes have been considered the most representative of this study being the ones where the effect of EP addition induces evident changes in mechanical performances and thermal conductivity. Increasing the first 24 h curing temperature up to $85 \text{ }^\circ\text{C}$ results in a decrease in geometric density, thus leading to an optimization in the light-weighting for both M-5EP and M-10EP. At the same time, water absorption increases thus indicating an increase in open porosity, as depicted in pore size distribution measured by MIP

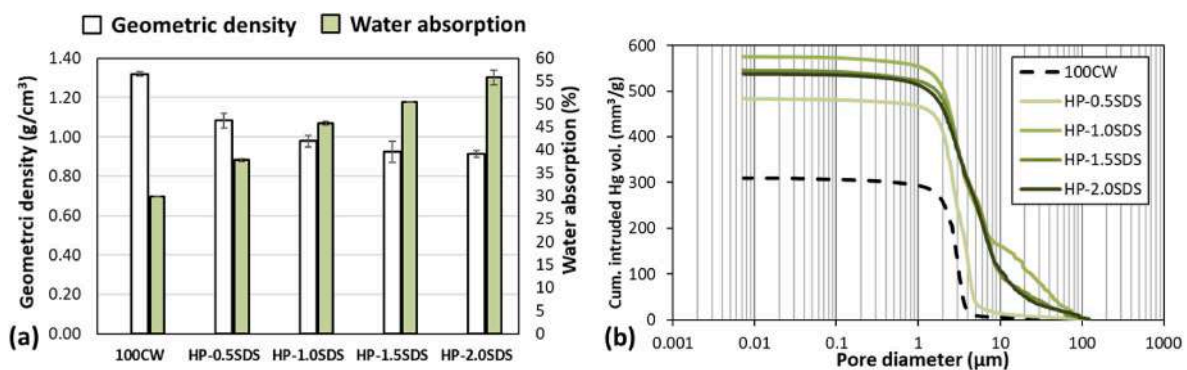


Fig. 4. (a) Geometric density, water absorption and (b) pore size distribution of the foam samples prepared with the combination of the pore stabilizing agent (SDS) in the concentration range of 0.5–2.0 and 1.0 wt% of hydrogen peroxide (HP).

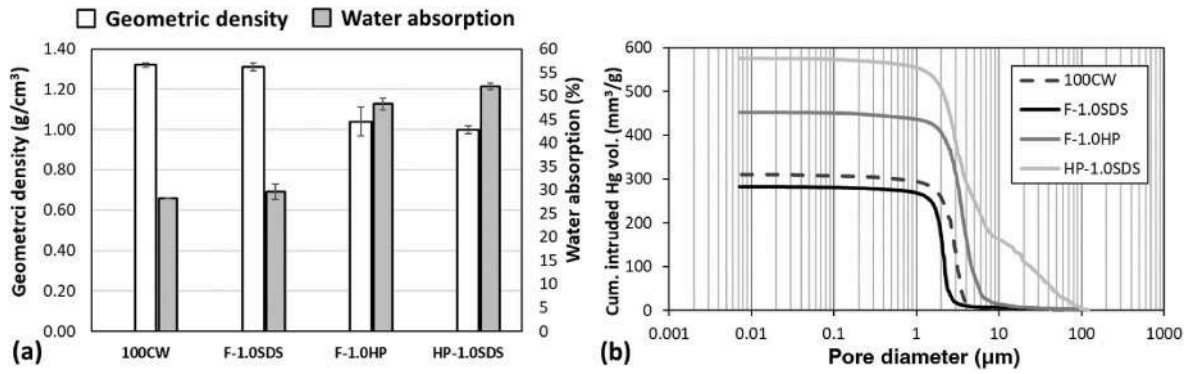


Fig. 5. Comparison of the physical properties ((a) geometric density and water absorption and (b) pore size distribution) among the reference unfoam sample (100CW) and the foams obtained by the addition of 1.0 wt% SDS (F-1.0SDS), 1.0 wt% hydrogen peroxide (F-1.0HP) and the combination of the previously mentioned agents (HP-1.0SDS).

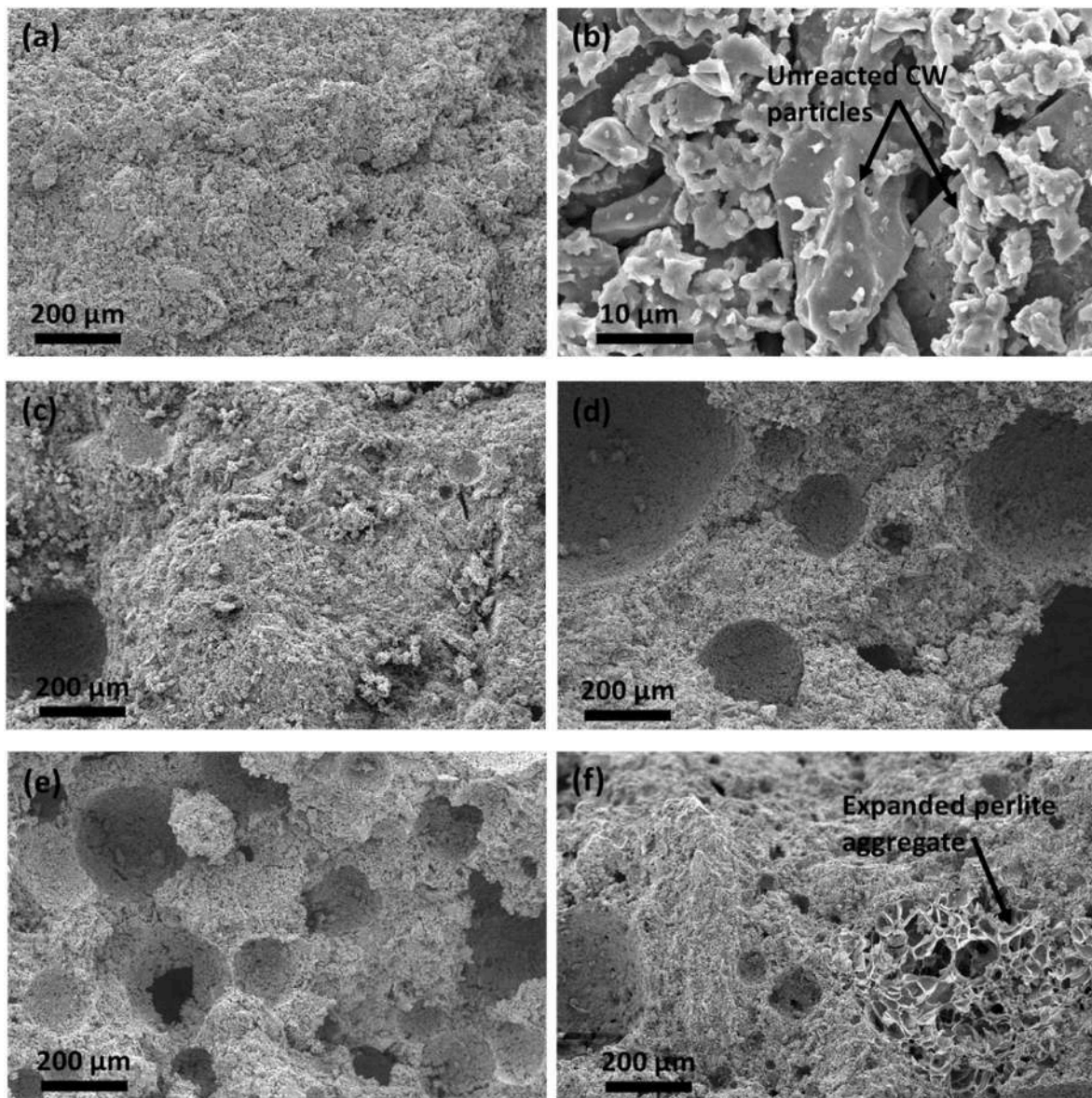


Fig. 6. SEM observation by secondary electrons of (a,b) the reference unfoam sample (100CW) at two different magnification and the foams obtained by the addition of (c) 1.0 wt% SDS (F-1.0SDS), (d) 1.0 wt% hydrogen peroxide (F-1.0HP), (e) the combination of the previously mentioned agents (HP-1.0SDS) and (f) the light-weight composite (M-5EP).

Table 5

Physical (geometric density and water absorption), mechanical (flexural and compressive strength) and thermal properties of lightweight composites with increasing expanded perlite content. Thermal conductivity of HP-1.0SDS foam is also reported as reference.

| Sample name | Geometric Density (ρ , g/cm ³) | Water absorption (WA, %) | Flexural strength (R_f , MPa) | Compressive strength (R_c , MPa) | Thermal conductivity (k , W/(m K)) |
|-------------|--|--------------------------|----------------------------------|-------------------------------------|---------------------------------------|
| HP-1.0SD | 1.00 ± 0.02 | 52.1 ± 0.7 | 1.1 ± 0.3 | 3.9 ± 0.3 | 0.484 ± 0.027 |
| M-5EP | 0.95 ± 0.02 | 51.8 ± 2.6 | 0.9 ± 0.2 | 3.1 ± 0.4 | 0.302 ± 0.022 |
| M-10EP | 0.75 ± 0.01 | 71.6 ± 0.7 | 0.6 ± 0.1 | 1.7 ± 0.1 | 0.258 ± 0.017 |
| M-13EP | 0.68 ± 0.02 | 83.8 ± 2.2 | 0.7 ± 0.1 | 1.7 ± 0.2 | 0.252 ± 0.043 |

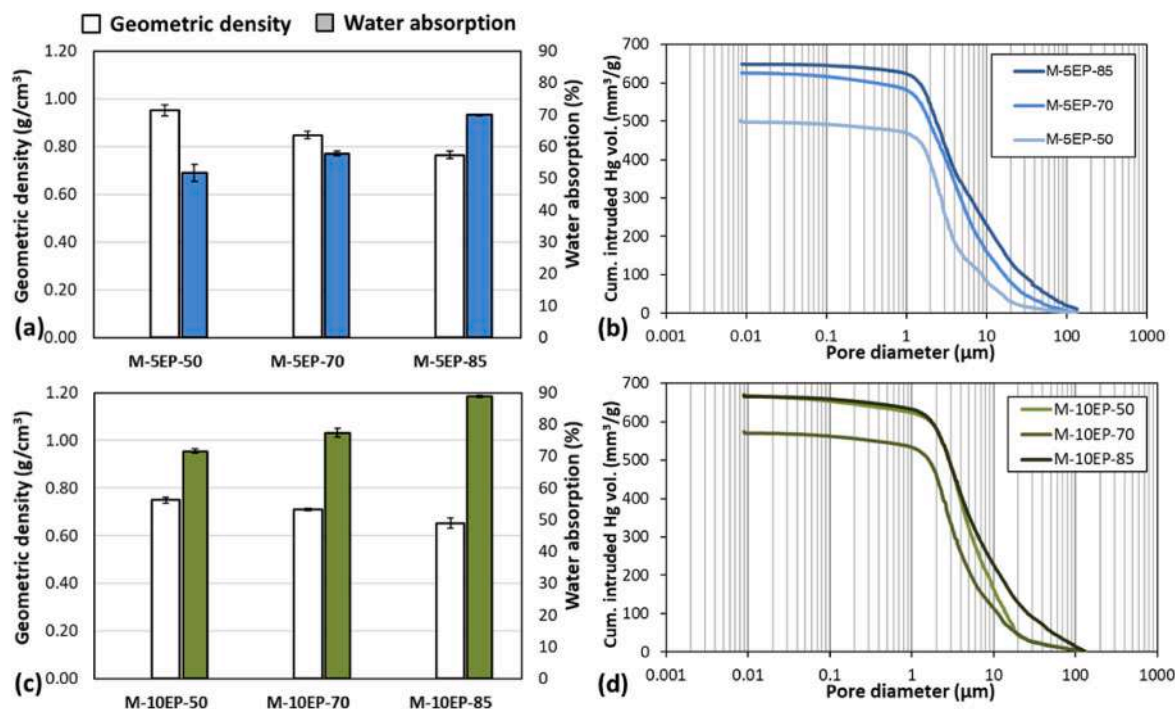


Fig. 7. Effect of curing temperature (50, 70 and 85 °C for the first 24h) on the physical properties of lightweight composites M-5EP (a, b) and M-10EP (c, d).

(Fig. 7c and d). These achievements in terms of geometric density and water absorption are related to the fact that increasing the temperature in the first 24h of curing, a higher yield in hydrogen peroxide decomposition and pores stabilization are promoted together with a faster geopolymerization [30]. Thus, besides the possibility to tune the expanded perlite content, these results demonstrate the possibility to improve the lightweight properties by optimizing the first 24 h curing temperatures, always considering conditions with $T < 100$ °C.

4. Conclusions

This study demonstrates that ceramic waste (CW), sourced from the rectifying process of porcelain stoneware tiles, can properly work as precursor in alkali activation systems and, with the addition of foaming agents and porous aggregates, there is the possibility to design lightweight composites. The main conclusions can be drawn as follows:

- it was demonstrated that CW is suitable for alkali activation also when used stand-alone (100 % CW). Theoretical molar ratios of Si/Al = 2.5, Na/Al = 1.0, Na/Si = 0.4 have been used to synthesize a stable alkali activated material with a density of 1.3 g/cm³ and a water absorption of 25 %;
- using 100 % CW, different direct foaming strategies have been tested by ranging the concentrations of pore stabilizing and foaming agents alone and/or in combination. Among the tested agents, hydrogen peroxide either alone either in combination with sodium dodecyl

sulfate induces the best performances. By adding both these agents in equal concentration (1.0 wt%), samples with a geometric density of 1.0 g/cm³ and a water absorption of 52 % have been obtained, with a homogenous pore distribution characterized by macro-pores;

- lightweight composites have been prepared by the addition of different content of expanded perlite and varying curing temperatures, as both these parameters have been found fundamental to tune the desired properties. It was found that the addition of 10 wt% of expanded perlite leads to samples with a geometric density of 0.75 g/cm³, a water absorption of 71.6 %, a compressive strength of 1.7 MPa, and a thermal conductivity of 0.26 W/mK. When the first 24 h of curing occurs at 85 °C, geometric density and water absorption are 0.65 g/cm³ and 88.8 %, respectively.

The possibility to synthesize lightweight composites by alkali activation of ceramic tiles waste has been demonstrated to be a feasible route and it can be considered a step forward towards the use of more sustainable materials in the industrial and building sector. The performances of the developed lightweight composites agree with data reported in the literature when conventional precursors for alkali activation are applied [26] and with cementitious foams based on magnesium silicates (e.g. Air Krete®), exhibiting thermal conductivity around 0.25 W/mK. A further step in research will be necessary, if lightweight composites performances wish to reach the thermal insulation values characteristics of materials such as fiberglass, mineral wool, polystyrene, which are lower of at least one order of magnitude.

CRediT authorship contribution statement

Giulia Masi: Writing – original draft, Methodology, Investigation, Data curation, Conceptualization. **Alessandro Tugnoli:** Writing – review & editing, Methodology, Investigation, Formal analysis, Data curation. **Maria Chiara Bignozzi:** Writing – review & editing, Supervision, Project administration, Funding acquisition, Conceptualization.

Declaration of competing interest

The authors declare that they have no known competing financial interests or personal relationships that could have appeared to influence the work reported in this paper.

Acknowledgements

This study was performed within the scope of the “Product and process sustainability for the production of tiles” project in the framework of Programma Operativo Nazionale (PON) “Ricerca e Innovazione” 2014–2020 (ai sensi dell’art. 24, comma 3, lett. a), della Legge 30 dicembre 2010, n. 240 e s.m.i. e del D.M. 10 agosto 2021 n. 106) of the Italian Ministry of University and Research (green thematic area). The Authors would like to acknowledge Chiara Benni for collaboration in sample preparation and materials characterizations.

Appendix A. Supplementary data

Supplementary data to this article can be found online at <https://doi.org/10.1016/j.ceramint.2024.10.399>.

References

- [1] S.A. Bernal, E.D. Rodríguez, A.P. Kirchheim, J.L. Provis, Management and valorisation of wastes through use in producing alkali-activated cement materials, *J. Chem. Technol. Biotechnol.* 91 (2016) 2365–2388, <https://doi.org/10.1002/jctb.4927>.
- [2] B. Ren, Y. Zhao, H. Bai, S. Kang, T. Zhang, S. Song, Eco-friendly geopolymer prepared from solid wastes: a critical review, *Chemosphere* 267 (2021) 128900, <https://doi.org/10.1016/j.chemosphere.2020.128900>.
- [3] J.L. Provis, Alkali-activated materials, *Cement Concr. Res.* 114 (2018) 40–48, <https://doi.org/10.1016/j.cemconres.2017.02.009>.
- [4] B.C. McLellan, R.P. Williams, J. Lay, A. van Riessen, G.D. Corder, Costs and carbon emissions for geopolymer pastes in comparison to ordinary Portland cement, *J. Clean. Prod.* 19 (2011) 1080–1090, <https://doi.org/10.1016/j.jclepro.2011.02.010>.
- [5] S. Fu, J. Lee, Recycling of ceramic tile waste into construction materials, *Develop. Built Environ.* 18 (2024) 100431, <https://doi.org/10.1016/j.dibe.2024.100431>.
- [6] R. Vilas Meena, J. Kumar Jain, H. Singh Chouhan, A. Singh Beniwal, Use of waste ceramics to produce sustainable concrete: a review, *Cleaner Mater.* 4 (2022) 100085, <https://doi.org/10.1016/j.clema.2022.100085>.
- [7] L. Reig, M.M. Tashima, L. Soriano, M. V Borrachero, J. Monzó, J. Payá, Alkaline activation of ceramic waste materials, *Waste Biomass Valor* 4 (2013) 729–736, <https://doi.org/10.1007/s12649-013-9197-z>.
- [8] H. Dahlbo, J. Bachér, K. Lähinen, T. Jouttijärvi, P. Suoheimo, T. Mattila, S. Sironen, T. Myllymaa, K. Saramäki, Construction and demolition waste management - a holistic evaluation of environmental performance, *J. Clean. Prod.* 107 (2015) 333–341, <https://doi.org/10.1016/j.jclepro.2015.02.073>.
- [9] L. Reig, M.M. Tashima, M. V Borrachero, J. Monzó, C.R. Cheeseman, J. Payá, Properties and microstructure of alkali-activated red clay brick waste, *Construct. Build. Mater.* 43 (2013) 98–106, <https://doi.org/10.1016/j.conbuildmat.2013.01.031>.
- [10] M. Tuyan, Ö. Andiç-Çakır, K. Ramyar, Effect of alkali activator concentration and curing condition on strength and microstructure of waste clay brick powder-based geopolymer, *Compos. B Eng.* 135 (2018) 242–252, <https://doi.org/10.1016/j.compositesb.2017.10.013>.
- [11] R.A. Robayo, A. Mulford, J. Munera, R. Mejía de Gutiérrez, Alternative cements based on alkali-activated red clay brick waste, *Construct. Build. Mater.* 128 (2016) 163–169, <https://doi.org/10.1016/j.conbuildmat.2016.10.023>.
- [12] E. Sassoni, P. Pahlavan, E. Franzoni, M.C. Bignozzi, Valorization of brick waste by alkali-activation: a study on the possible use for masonry repointing, *Ceram. Int.* 42 (2016) 14685–14694, <https://doi.org/10.1016/j.ceramint.2016.06.093>.
- [13] M. Fugazzotto, G. Cultrone, P. Mazzoleni, G. Barone, Suitability of ceramic industrial waste recycling by alkaline activation for use as construction and restoration materials, *Ceram. Int.* (2022), <https://doi.org/10.1016/j.ceramint.2022.11.111>.
- [14] B. Horvat, V. Ducman, Potential of green ceramics waste for alkali activated foams, *Materials* 12 (2019), <https://doi.org/10.3390/ma12213563>.
- [15] Z. Bayer Ozturk, R. Çirik, I.I. Atabey, Sustainable environment approach by the usage of ceramic pottery waste in geopolymer mortar, *Int. J. Environ. Sci. Technol.* 20 (2023) 7577–7588, <https://doi.org/10.1007/s13762-023-04939-0>.
- [16] L. Carabba, S. Manzi, E. Rambaldi, G. Ridolfi, M.C. Bignozzi, High-temperature behaviour of alkali-activated composites based on fly ash and recycled refractory particles, *J. Ceram. Sci. Technol.* 8 (2017) 377–387, <https://doi.org/10.4416/JCST2017-00047>.
- [17] S.A. Bernal, J. Bejarano, C. Garzón, R. Mejía De Gutiérrez, S. Delvasto, E. D. Rodríguez, Performance of refractory aluminosilicate particle/fiber-reinforced geopolymer composites, *Compos. B Eng.* 43 (2012) 1919–1928, <https://doi.org/10.1016/j.compositesb.2012.02.027>.
- [18] E.D. Yanti, L. Mubarak, Subari, B.D. Erlangga, E. Widyaningsih, Jakah, I. Pratiwi, A. Rinovian, T. Nugroho, B. Herbudiman, Utilization of various ceramic waste as fine aggregate replacement into fly ash-based geopolymer, *Mater. Lett.* 357 (2024) 135651, <https://doi.org/10.1016/j.matlet.2023.135651>.
- [19] I. Luhar, S. Luhar, M.M.A.B. Abdullah, M. Nabiałek, A.V. Sandu, J. Szmidla, A. Jurdzinska, R.A. Razak, I.H.A. Aziz, N.H. Jamil, L.M. Deramanet, Assessment of the suitability of ceramic waste in geopolymer composites: an appraisal, *Materials* 14 (2021) 3279, <https://doi.org/10.3390/ma14123279>.
- [20] G. Boschi, G. Masi, G. Bonvicini, M.C. Bignozzi, Sustainability in Italian ceramic tile production: evaluation of the environmental impact, *ApplSci.* (Switzerland) 10 (2020) 1–15, <https://doi.org/10.3390/app10249063>.
- [21] G. Boschi, G. Bonvicini, G. Masi, M.C. Bignozzi, Recycling insight into the ceramic tile manufacturing industry, *Open Ceram.* 16 (2023) 100471, <https://doi.org/10.1016/j.oceram.2023.100471>.
- [22] L. Baraldi, World production and consumption of ceramic tiles, *Ceramic World Rev.* 153 (2023) 58–72, <https://www.acimac.it/area/centro-studi/documentazione/#servizi>.
- [23] M. Nodéhi, A comparative review on foam-based versus lightweight aggregate-based alkali-activated materials and geopolymer, *Innov. Infrastruct. Solution.* 6 (2021) 1–20, <https://doi.org/10.1007/s41062-021-00595-w>.
- [24] X. Li, C. Bai, Y. Qiao, X. Wang, K. Yang, P. Colombo, Preparation, properties and applications of fly ash-based porous geopolymers: a review, *J. Clean. Prod.* 359 (2022) 132043, <https://doi.org/10.1016/j.jclepro.2022.132043>.
- [25] M. Abdellatif, M.A. Elrahman, H. Alanazi, A.A. Abadel, A. Tahwia, A state-of-the-art review on geopolymer foam concrete with solid waste materials: components, characteristics, and microstructure, *Innov. Infrastruct. Solution.* 8 (2023) 230, <https://doi.org/10.1007/s41062-023-01202-w>.
- [26] R.M. Novais, R.C. Pullar, J.A. Labrincha, Geopolymer foams: an overview of recent advancements, *Prog. Mater. Sci.* 109 (2020), <https://doi.org/10.1016/j.pmatsci.2019.100621>.
- [27] C. Bai, P. Colombo, Processing, properties and applications of highly porous geopolymers: a review, *Ceram. Int.* 44 (2018) 16103–16118, <https://doi.org/10.1016/j.ceramint.2018.05.219>.
- [28] V. Medri, E. Papa, J. Dedecek, H. Jirglova, P. Benito, A. Vaccari, E. Landi, Effect of metallic Si addition on polymerization degree of in situ foamed alkali-aluminosilicates, *Ceram. Int.* 39 (2013) 7657–7668, <https://doi.org/10.1016/j.ceramint.2013.02.104>.
- [29] E. Kamseu, B. Nait-Ali, M.C. Bignozzi, C. Leonelli, S. Rossignol, D.S. Smith, Bulk composition and microstructure dependence of effective thermal conductivity of porous inorganic polymer cements, *J. Eur. Ceram. Soc.* 32 (2012) 1593–1603, <https://doi.org/10.1016/j.jeurceramsoc.2011.12.030>.
- [30] G. Masi, W. Rickard, L. Vickers, M.C. Bignozzi, A. van Riessen, A comparison between different foaming methods for the synthesis of light weight geopolymers, *Ceram. Int.* 40 (2014) 13891–13902, <https://doi.org/10.1016/j.ceramint.2014.05.108>.
- [31] G. Masi, W. Rickard, M.C. Bignozzi, A. Van Riessen, The effect of organic and inorganic fibres on the mechanical and thermal properties of aluminate activated geopolymers, *Compos. B Eng.* 76 (2015) 218–228, <https://doi.org/10.1016/j.compositesb.2015.02.023>.
- [32] V. Ducman, L. Korat, Characterization of geopolymer fly-ash based foams obtained with the addition of Al powder or H₂O₂ as foaming agents, *Mater. Char.* 113 (2016) 207–213, <https://doi.org/10.1016/j.matchar.2016.01.019>.
- [33] Z. Abdollahnejad, S. Miraldo, F. Pacheco-Torgal, J.B. Aguiar, Cost-efficient one-part alkali-activated mortars with low global warming potential for floor heating systems applications, *Eur. J. Environ. Civil Eng.* 21 (2017) 412–429, <https://doi.org/10.1080/19648189.2015.1125392>.
- [34] P. Hlaváček, V. Šmilauer, F. Škvára, L. Kopecký, R. Šulc, Inorganic foams made from alkali-activated fly ash: mechanical, chemical and physical properties, *J. Eur. Ceram. Soc.* 35 (2015) 703–709, <https://doi.org/10.1016/j.jeurceramsoc.2014.08.024>.
- [35] B. Qin, Y. Lu, F. Li, Y. Jia, C. Zhu, Q. Shi, Preparation and stability of inorganic solidified foam for preventing coal fires, *Adv. Mater. Sci. Eng.* 2014 (2014), <https://doi.org/10.1155/2014/347386>.
- [36] L. Korat, V. Ducman, The influence of the stabilizing agent SDS on porosity development in alkali-activated fly-ash based foams, *Cem. Concr. Compos.* 80 (2017) 168–174, <https://doi.org/10.1016/j.cemconcomp.2017.03.010>.
- [37] G. Indu Siva Ranjani, K. Ramamurthy, Analysis of the foam generated using surfactant sodium lauryl sulfate, *Int. J. Concr. Struct. Mater.* 4 (2010) 55–62, <https://doi.org/10.4334/ijcsm.2010.4.1.055>.
- [38] L. Carabba, R. Moricone, G.E. Scarponi, A. Tugnoli, M.C. Bignozzi, Alkali activated lightweight mortars for passive fire protection: a preliminary study, *Construct. Build. Mater.* 195 (2019) 75–84, <https://doi.org/10.1016/j.conbuildmat.2018.11.005>.

- [39] L. Carabba, S. Pirskawetz, S. Krüger, G. Gluth, M.C. Bignozzi, Acoustic emission study of heat-induced cracking in fly ash-based alkali-activated pastes and lightweight mortars, *Cem. Concr. Compos.* 102 (2019) 145–156, <https://doi.org/10.1016/j.cemconcomp.2019.04.013>.
- [40] A. Bonilla, M.A. Villaquirán-Cacedo, R. Mejía de Gutiérrez, Novel alkali-activated materials with photocatalytic and bactericidal properties based on ceramic tile waste, *Coatings* 12 (2022) 35, <https://doi.org/10.3390/coatings12010035>.
- [41] L. Soriano, M.M. Tashima, L. Reig, J. Payá, M.V. Borrachero, J.M. Monzó, Á. M. Pitarch, Reusing ceramic waste as a precursor in alkali-activated cements: a review, *Buildings* (Switzerland) 13 (2023) 3022, <https://doi.org/10.3390/buildings13123022>.
- [42] M. Fugazzotto, P. Mazzoleni, A. Stroschio, G. Barone, Creating mortars through the alkaline activation of ceramic waste from construction: case studies on their applicability and versatility in conservation, *Sustainability* 16 (2024) 1085, <https://doi.org/10.3390/su16031085>.
- [43] Y. Zheng, C. Sun, C. Qiu, S. Wu, F. Rao, L. Yang, Addition of ceramic waste for the preparation of VA-based alkali-activated material with high temperature resistance, *J. Build. Eng.* 82 (2024) 108385, <https://doi.org/10.1016/j.job.2023.108385>.
- [44] Y. Liang, Q. Wang, W. Gan, J. Liao, M. Lai, J. Ho, A 14-year study on ceramic waste slag-based lightweight aggregate concrete, *Construct. Build. Mater.* 330 (2022) 127152, <https://doi.org/10.1016/j.conbuildmat.2022.127152>.
- [45] F. Aredes, T. Campos, J. MacHado, K. Sakane, G. Thim, D. Brunelli, Effect of cure temperature on the formation of metakaolinite-based geopolymer, *Ceram. Int.* 41 (2015) 7302–7311, <https://doi.org/10.1016/j.ceramint.2015.02.022>.
- [46] M. Nodehi, T. Ozbakkaloglu, A. Gholampour, T. Mohammed, X. Shi, The effect of curing regimes on physico-mechanical, microstructural and durability properties of alkali-activated materials: a review, *Construct. Build. Mater.* 321 (2022) 126335, <https://doi.org/10.1016/j.conbuildmat.2022.126335>.
- [47] M.C. Bignozzi, S. Manzi, M.E. Natali, W.D.A. Rickard, A. Van Riessen, Room temperature alkali activation of fly ash: the effect of $\text{Na}_2\text{O}/\text{SiO}_2$ ratio, *Construct. Build. Mater.* 69 (2014) 262–270, <https://doi.org/10.1016/j.conbuildmat.2014.07.062>.
- [48] G. Masi, Steel corrosion behavior in light weight fly-ash based Alkali activated mortars, *ApplSci.* (Switzerland) 11 (2021) 1–13, <https://doi.org/10.3390/app11041908>.
- [49] G. Masi, A. Filippini, M.C. Bignozzi, Fly ash-based one-part alkali activated mortars cured at room temperature: effect of precursor pre-treatments, *Open Ceram.* 8 (2021) 100178, <https://doi.org/10.1016/j.oceram.2021.100178>.
- [50] W.D.A. Rickard, R. Williams, J. Temuujin, A. van Riessen, Assessing the suitability of three Australian fly ashes as an aluminosilicate source for geopolymers in high temperature applications, *Mater. Sci. Eng.* 528 (2011) 3390–3397, <https://doi.org/10.1016/j.msea.2011.01.005>.
- [51] L. Gouissem, A. Benmekideche, Contribution to the expansion of low density polyethylene by the use of chemical blowing agents based on sodium bicarbonate and/or citric acid, *Polym. Sci. Series A* 63 (2021) 542–555, <https://doi.org/10.1134/S0965545X21050059>.
- [52] T. Sadik, C. Pillon, C. Carrot, J. Reglero Ruiz, Dsc studies on the decomposition of chemical blowing agents based on citric acid and sodium bicarbonate, *Thermochim. Acta* 659 (2018) 74–81, <https://doi.org/10.1016/j.tca.2017.11.007>.
- [53] EN 1015-3:1999 Methods of test for mortar for masonry. Determination of Consistence of Fresh Mortar (By Flow Table).
- [54] C.R. Kaze, H.K. Tchakoute, T.T. Mbakop, J.R. Mache, E. Kamseu, U.C. Melo, C. Leonelli, H. Rahier, Synthesis and properties of inorganic polymers (geopolymers) derived from Cameroon-meta-halloysite, *Ceram. Int.* 44 (15) (2018) 18499–18508, <https://doi.org/10.1016/j.ceramint.2018.07.070>.
- [55] EN 196-1:2016 Methods of Testing Cement - Part 1, Determination of strength, 2016.
- [56] ISO 22007-2:2015, *Plastics - Determination of Thermal Conductivity and Thermal Diffusivity -Part 2: Transient Plane Heat Source (Hot Disc) Method*, 2015.
- [57] M. Gustavsson, S.E. Gustafsson, On the use of transient plane source sensors for studying materials with direction dependent properties, in: *Proceedings of 26th ITCC, 6–8 August 2011, 2011*. Cambridge, USA.
- [58] S.E. Gustafsson, Transient plane source techniques for thermal conductivity and thermal diffusivity measurements of solid materials, *Rev. Sci. Instrum.* 62 (1991) 797–804.
- [59] P. Rovnaník, Effect of curing temperature on the development of hard structure of metakaolin-based geopolymer, *Construct. Build. Mater.* 24 (2010) 1176–1183, <https://doi.org/10.1016/j.conbuildmat.2009.12.023>.
- [60] J.L. Provis, P. Duxson, J.S.J. van Deventer, The role of particle technology in developing sustainable construction materials, *Adv. Powder Technol.* 21 (2010) 2–7, <https://doi.org/10.1016/j.apt.2009.10.006.38>.
- [61] L. Carabba, G. Masi, S. Pirskawetz, S. Krüger, G. Gluth, M.C. Bignozzi, Thermal properties and steel corrosion in light-weight alkali activated mortars, in: *International Conference on Sustainable Materials, Systems and Structures (SMSS 2019) New Generation of Construction Materials*, 2019, pp. 125–132.